

This article was downloaded by:

On: 15 January 2011

Access details: *Access Details: Free Access*

Publisher *Taylor & Francis*

Informa Ltd Registered in England and Wales Registered Number: 1072954 Registered office: Mortimer House, 37-41 Mortimer Street, London W1T 3JH, UK



Comments on Inorganic Chemistry

Publication details, including instructions for authors and subscription information:

<http://www.informaworld.com/smpp/title~content=t713455155>

X-Ray Absorption

To cite this Article (1984) 'X-Ray Absorption', *Comments on Inorganic Chemistry*, 3: 5, 261 – 272

To link to this Article: DOI: 10.1080/02603598408080076

URL: <http://dx.doi.org/10.1080/02603598408080076>

PLEASE SCROLL DOWN FOR ARTICLE

Full terms and conditions of use: <http://www.informaworld.com/terms-and-conditions-of-access.pdf>

This article may be used for research, teaching and private study purposes. Any substantial or systematic reproduction, re-distribution, re-selling, loan or sub-licensing, systematic supply or distribution in any form to anyone is expressly forbidden.

The publisher does not give any warranty express or implied or make any representation that the contents will be complete or accurate or up to date. The accuracy of any instructions, formulae and drug doses should be independently verified with primary sources. The publisher shall not be liable for any loss, actions, claims, proceedings, demand or costs or damages whatsoever or howsoever caused arising directly or indirectly in connection with or arising out of the use of this material.

V. X-RAY ABSORPTION

A. Basic Principles

Figure V-1 contains a more extended region of the molecular energy level diagram for D_{4h} - CuCl_4^- . If the absorption spectrum is scanned to energies higher than those of the charge-transfer transitions, we would next expect to observe transitions associated with an electron

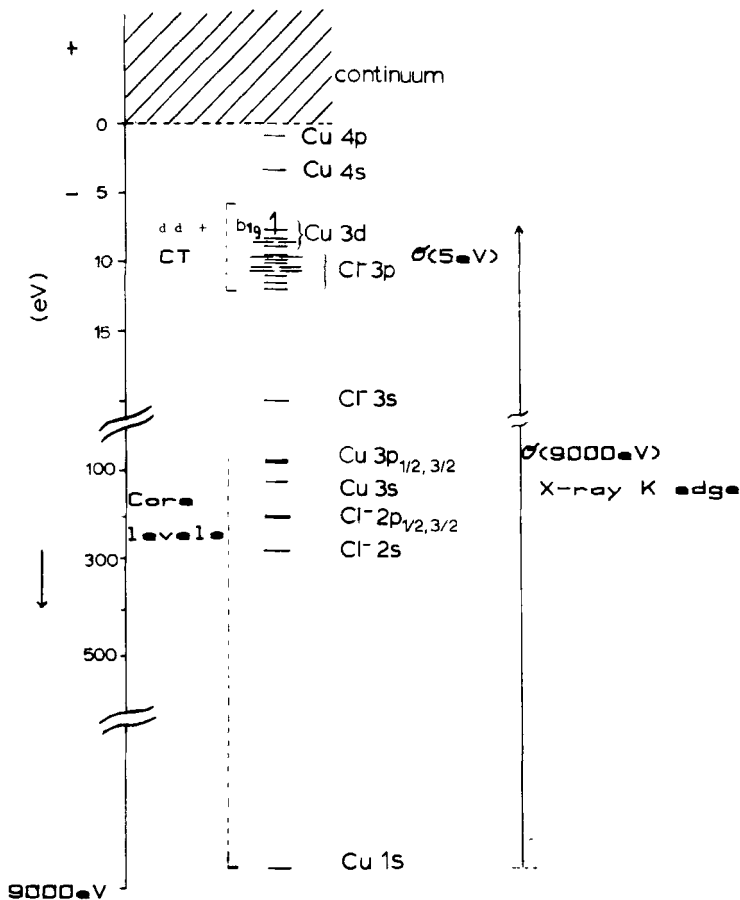


FIGURE V-1 Energy level diagram for D_{4h} - CuCl_4^- : Extended from Figure IV-2 (left). All core, CT and d levels are filled, with the exception of b_{1g} , which has one unpaired electron.

being excited from the $3d$ orbitals into the $4s$ and $4p$ unoccupied levels on the copper. Since the copper $4s$ and $4p$ are valence orbitals which can mix with the ligand $3p$ and copper $3d$ orbitals, their direct spectroscopic study is quite important in evaluating their participation in bonding. Unfortunately, the spectroscopic region above $\sim 55,000\text{ cm}^{-1}$ ($\sim 7\text{ eV}$ where $1\text{ eV} = 8066\text{ cm}^{-1}$) is quite difficult to probe experimentally. Since most molecules absorb strongly in this region, it can be difficult to find a spectroscopically transparent host and counter-ion. In addition, a VUV (vacuum ultraviolet) spectrometer is required. The most useful continuous energy source of photons in this range and into the x-ray region is synchrotron radiation from a storage ring (as described in Section B). The ring is maintained at ultrahigh vacuum (UHV) with Be windows transmitting photons at energies above $\sim 3000\text{ eV}$. In the region between 7 and 3000 eV , Be windows absorb, thus the experiment must be contained in UHV. Few systematic absorption studies on inorganic complexes have been performed in this region.¹ Above 3000 eV , core electrons are excited at energies which are well separated for different atoms, and transitions on a specific atom of interest can be observed. Studies in this x-ray region will probe the open valence $4s$ and $4p$ (as well as the highest energy half-occupied $3d$) levels on the copper, but at lower resolution ($\sim 1.5\text{ eV}$ as compared to $\sim 0.01\text{ eV}$ in vacuum UV spectroscopy) due to intrinsic lifetime broadening as well as lower monochromator resolution at these high energies.

The copper K -edge absorption spectrum starting at energies near 9000 eV corresponds to excitation of an electron from the filled $1s$ orbital into bound levels and the continuum. This x-ray spectrum is usually considered in two regions as shown in Figure V-2. At high energy the EXAFS (extended x-ray absorption fine structure) region gives structural information on the atoms adjacent to the copper center (number, type and bond length; see recent reviews).² In this spectroscopic overview we focus on the lower energy region of the spectrum, the absorption edge which directly relates to the energy level diagram in Figure V-1. For x-ray absorption spectroscopy,³ we are again interested in a transition moment integral [Eq. (III-1b)] of the form $\int \psi_g \hat{M} \psi_e d\tau$ which reduces to a one-electron integral over the orbital in the ground state and in the excited state involved in the transition. For the K edge, ψ_g involves the electron in the $1s$ orbital. The ψ_e , associated with the lowest energy part of the edge, results from excitation of this electron into unoccupied bound levels

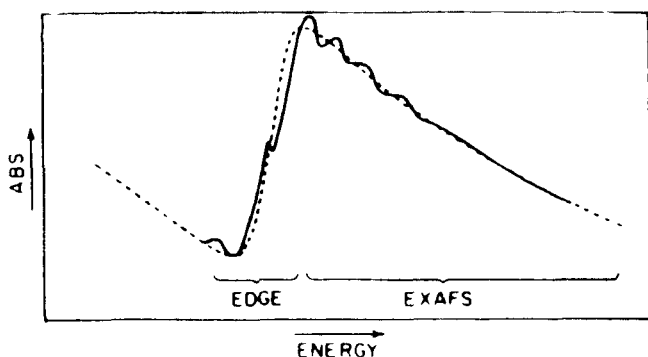


FIGURE V-2 K edge x-ray absorption spectrum.

in Figure V-1 ($E < 0$), while the absorption at higher energies in the edge region corresponds to the $1s$ electron being ionized into the continuum of unbound states with $E > 0$. For an electric dipole transition, excitation of a $1s$ electron into the bound $3d$ or $4s$ open levels of $D_{4h}\text{-CuCl}_4^-$ is forbidden, while $1s \rightarrow 4p$ is allowed, as is excitation to higher bound Rydberg levels (np with $n > 4$). However, these higher Rydberg levels involve very diffuse wavefunctions which have poor overlap with the localized core $1s$ orbital and hence have low absorption intensity. Alternatively, transition intensity for excitation of a $1s$ electron into the continuum is at its maximum value for energies near zero and decreases with increasing energy. Further, certain of the lower energy states in the continuum can have their wavefunctions localized within the molecule. This is due to the interaction of the negative potential of the ligands with the unbound photoelectron, and produces significant overlap of this unbound state with the $1s$ orbital. This leads to an intense and sharp transition in the low energy region of the continuum called a "shape resonance" which can also contribute to the structure in the edge region.⁴ Thus assignment of the structure in the x-ray absorption edge is complex but important in probing bonding and requires detailed spectral study as outlined in the next section.

B. The Experiment

The main experimental feature of x-ray absorption spectroscopy which should be mentioned is the use of synchrotron radiation⁵ at facilities such as SSRL at Stanford. This has revolutionized x-ray

spectroscopy (as well as photoelectron spectroscopy, see Section VI) as it provides a high intensity continuous energy source of photons from the far IR to the x-ray region which peaks in intensity at x-ray energies (Figure V-3). This radiation is produced by electrons at relativistic energies (~ 3 GeV) moving in a UHV ($\leq 10^{-9}$ torr) storage ring in paths bent by a magnetic field. These electrons radiate, tangential to the electron orbit, a collimated cone of photons polarized in the orbital plane (see Figure V-3).

Two types of x-ray absorption edge spectral studies on copper complexes have been pursued. The first is a more empirical correlation

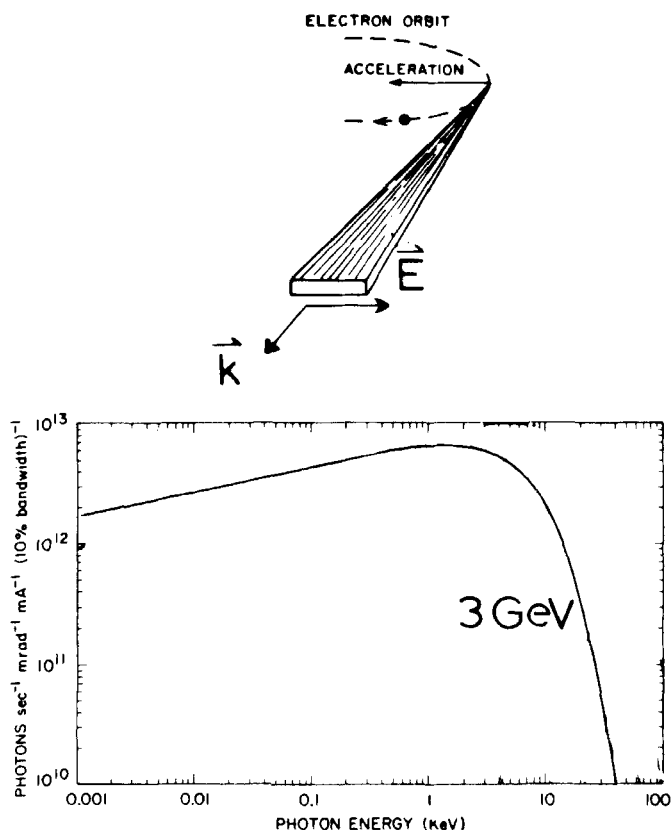


FIGURE V-3 Characteristics of synchrotron radiation: Polarization and propagation (top), energy distribution of intensity (bottom) (taken from Ref. 5).

of the energy and shape of the x-ray edge with oxidation state and geometry.⁶ From the energy level diagram in Figure V-1, reduction to Cu(I) will eliminate the possibility of a $(1s)^2 \dots (3d)^9 \rightarrow (1s)^1 \dots (3d)^{10}$ transition, and should also shift the 1s and copper valence orbitals to lower energy due to the reduction in effective nuclear charge. However, a change in geometry should only affect the valence orbitals. While changes in valence orbital energies with geometry may not be resolvable by this technique, absorption intensity can be strongly affected, through changes in mixing among the valence wavefunctions. This is particularly important in the case of a noncentrosymmetric distortion which can mix the electric dipole allowed $1s \rightarrow 4p$ transition into the electric dipole forbidden $1s \rightarrow 3d$ and $1s \rightarrow 4s$ transitions. The x-ray absorption edges^{6a} of a representative Cu(I) and Cu(II) complex are shown in Figure V-4. The edge region of the Cu(I) complex is shifted to lower energy with an

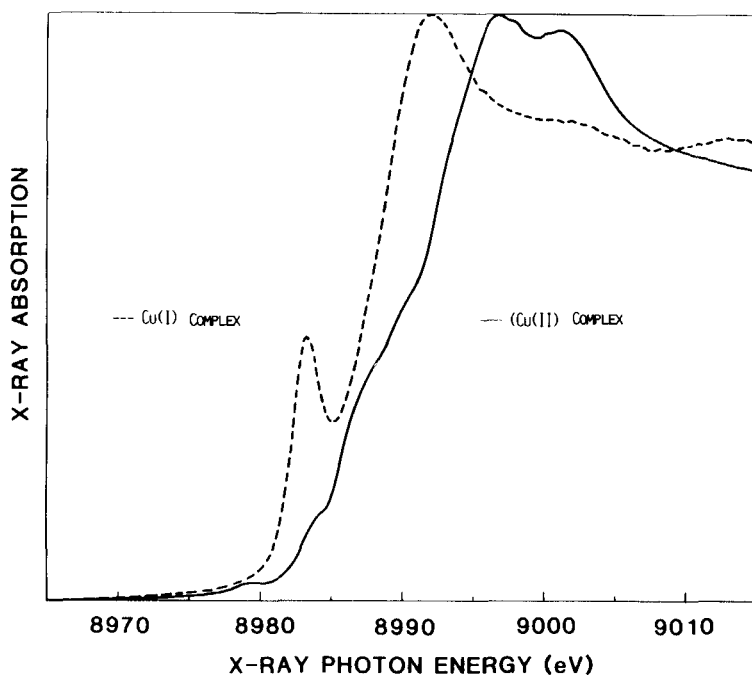


FIGURE V-4 X-ray absorption edges of representative Cu(I) and Cu(II) complexes.

intense transition at 8984 eV and an edge maximum at 8992 eV. For Cu(II) complexes a very weak transition is observed at 8979 eV with an intense edge maximum at 9000 eV. If the x-ray absorption edge spectra are normalized and that of a Cu(I) complex has subtracted from it the edges of a variety of different Cu(II) complexes, the spectra shown in Figure V-5 are obtained.^{6b} These normalized difference edge spectra are observed to be fairly insensitive to the nature of the copper complex and provide a technique for analytically determining the amount of Cu(I) present in an unknown sample.

On a more spectroscopic level, of the features observed in the x-ray absorption edge spectra of copper complexes (Figure V-4), only the weak feature at 8979 eV in Cu(II) complexes has been definitely assigned.⁷ This has been accomplished by polarized single

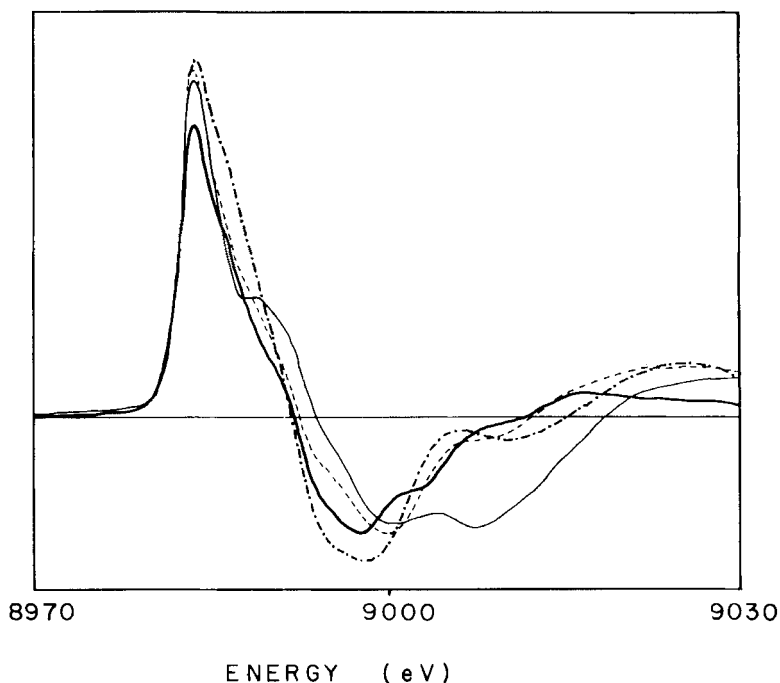


FIGURE V-5 Normalized difference edge spectra: One Cu(I) model (N_2S coordination) minus a variety of Cu(II) models (N_4O_1 (—,---); N_2O_2 (- - -); and N_2O_2S (—) coordinations).

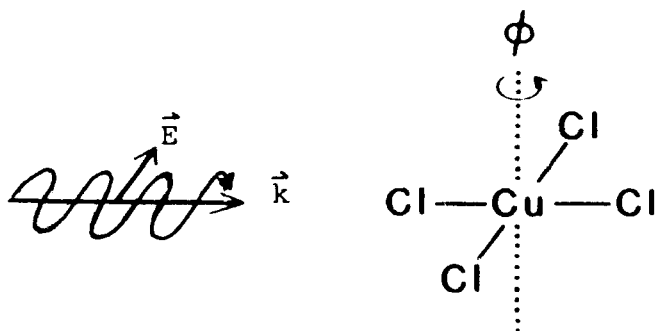


FIGURE V-6 Polarized single crystal x-ray absorption experiment: \vec{E} is the polarization direction of light, \vec{k} the propagation direction, and ϕ the angle of rotation of $D_{4h}\text{-CuCl}_4$ about the z axis ($\equiv 0^\circ$ along a Cl-Cu bond).

crystal x-ray absorption studies on $D_{4h}\text{-CuCl}_4$. In this experiment, x-rays were propagated, normal to the molecular z axis, with the \vec{E} vector oriented in the equatorial plane as shown in Figure V-6. When the crystal was rotated by an angle ϕ about the molecular z axis, the polarized x-ray absorption edge spectrum changed, Figure V-7. In particular, the weak peak at 8979 eV is essentially absent when the \vec{E} vector is along the Cl-Cu axis ($\phi = 0^\circ$) but appears when the complex is rotated away from this orientation. The intensity of this peak for a number of angles of rotation ϕ is plotted in Figure V-8. This intensity pattern allows a definitive assignment of this transition as discussed in the next section.

C. Comparison of Experiment and Theory

Thus far we have considered only the electric dipole operator ($\vec{M}(x,y,z)$) in the multipole expansion in Eq. III-2. If the 8979 eV transition obeyed electric dipole selection rules in D_{4h} , Figure V-8 (where \vec{E} is parallel to the molecular x,y axes) would either exhibit no intensity for all ϕ for a z polarized transition, or nonzero intensity which is constant with ϕ for an (x,y) polarized degenerate transition. The fact that the intensity of the transition peaks every 90° when the propagation direction of the light bisects the Cl-Cu-Cl bonds requires this to be an electric quadrupole transition. The expression for the electric quadrupole transition moment integral is given in Eq. (V-1), where \vec{E} is the polarization vector of the incoming x-ray with prop-

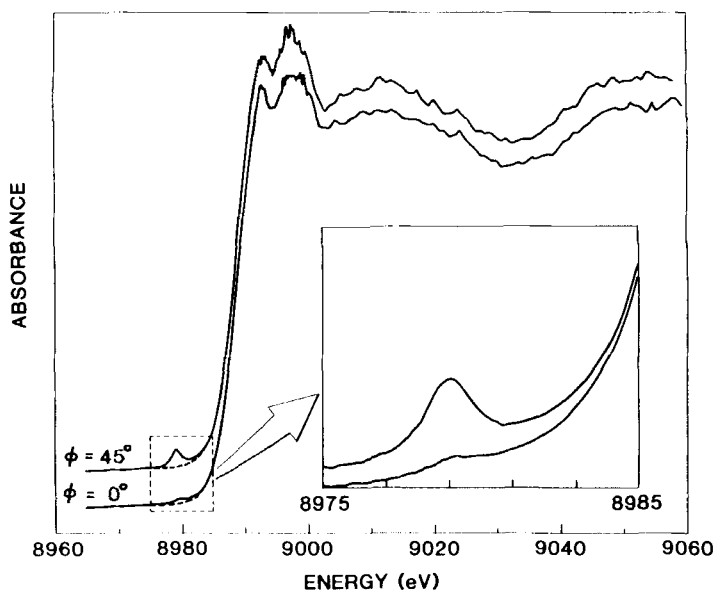


FIGURE V-7 Polarized single crystal x-ray absorption spectrum of D_{4h} - CuCl_4^{2-} . ϕ defined in Figure V-6. Insert gives 8979 eV peak at higher sensitivity.

agation direction \vec{k} , and \vec{p} and \vec{r} are the electron momentum and coordinate operators

$$f_{\text{electric quadrupole}} \propto \langle 1s | (\vec{E} \cdot \vec{p})(\vec{k} \cdot \vec{r}) | \psi_e \rangle \quad (\text{V-1})$$

Defining \vec{E} along x and \vec{k} along y , the electric quadrupole operator transforms as $M(xy)$. This operator will allow a transition from the $1s$ orbital to an excited state which also transforms as xy in the coordinate system defined by \vec{E} and \vec{k} . This is just the case for a $d_{x^2-y^2}$ orbital when the lobes are oriented at 45° to the propagation direction, the orientation of maximum experimental absorption intensity in Figure V-8. Thus we can assign the 8979 eV peak as a $1s \rightarrow 3d_{x^2-y^2}$ transition induced by the higher quadrupole term in Eq. (III-2). This term is active for two reasons: (1) the $1s \rightarrow 3d$ transition is electric dipole forbidden in D_{4h} and, (2) at 9000 eV the wavelength of the photon is $\sim 1.4 \text{ \AA}$ which is no longer large relative to the

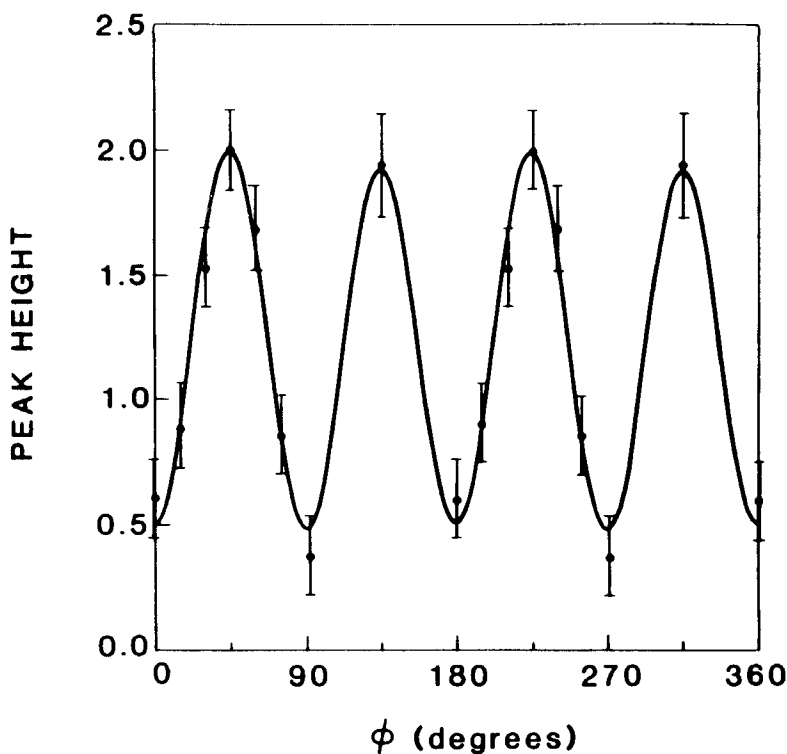


FIGURE V-8 Intensity of 8979 eV peak as a function of ϕ .

orbital of the electron, hence higher terms in the multipole expansion might be expected to make significant contributions.

If the D_{4h} - CuCl_4^- complex is distorted to the D_{2d} - CuCl_4^- geometry, both the $3d_{x^2-y^2}$ and $4p_z$ orbitals have b_2 symmetry and thus are allowed to mix by group theory. Significant p_z mixing (12%) into the $3d_{x^2-y^2}$ ground state has been proposed⁸ as an explanation for the small copper hyperfine splitting observed in the EPR spectrum of D_{2d} - CuCl_4^- . Since the $1s \rightarrow 4p_z$ transition is electric dipole allowed, this mixing would induce electric dipole character into the $1s \rightarrow 3d_{x^2-y^2}$ transition in the copper K edge. Experimentally⁹ (Figure V-9) the 8979 eV transition increases in intensity in the D_{2d} - CuCl_4^- geometry by a factor of ~ 4 . SCF-X α -SW calculations on D_{2d} - CuCl_4^- indicate that there is approximately the same amount of $d_{x^2-y^2}$ char-

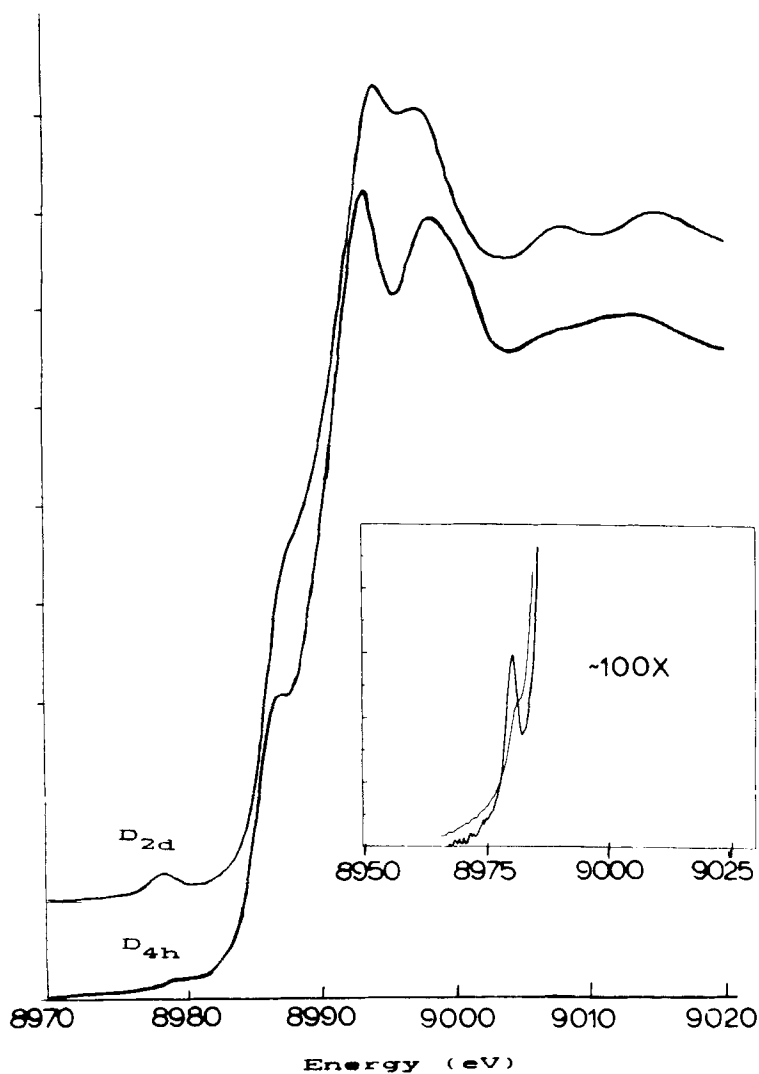


FIGURE V-9 Comparison of normalized x-ray absorption edge spectra of D_{4h} and D_{2d} CuCl_4^- . Insert gives 8979 eV peak at higher sensitivity.

acter in the ground state as found for D_{4h} -CuCl₄⁼ in Section II-C. Thus the increase in intensity must be due to Cu 4*p_z* mixing. (Note that ligand character mixed into the $d_{x^2-y^2}$ orbital cannot directly contribute to transition intensity as this has essentially no overlap with the Cu 1*s* orbital.) The SCF-X α -SW calculations indicate 2.1% *p_z* mixing into the $d_{x^2-y^2}$ ground state in D_{2d} -CuCl₄⁼. Using this value of *p_z* mixing and the experimental 8979 eV intensity in Figure V-9, one estimates the relative magnitudes of pure $1s \xrightarrow{M(xy)} d_{x^2-y^2}$ and $1s \xrightarrow{M(z)} 4p_z$ transitions to be $\sim 1:100$, which appears to be reasonable for terms in the multipole expansion at this wavelength.¹⁰ However, 2.1% *p_z* mixing is not consistent with the present interpretation of the copper hyperfine splitting in D_{2d} -CuCl₄⁼. Ideally, one would like a direct experimental determination of the $1s \xrightarrow{M(z)} 4p_z$ transition intensity to quantitate mixing [using Eq. (III-4)]. A possible assignment for the $1s \rightarrow 4p_z$ transition in the x-ray absorption spectrum is the peak at 8986 eV which is strongly *z* polarized.^{9,11} However, the alternative assignment of the 8986 eV peak as a "shake down" transition involving $1s \rightarrow 4p$ simultaneous with a Cl \rightarrow Cu(II) charge-transfer transition, made allowed by configurational interaction, has also been proposed.¹⁰ This is analogous to the satellite structure observed in XPS spectroscopy (see Section VIA). Further experiments are required to distinguish between these possibilities.

To summarize, the electric dipole forbidden $1s \rightarrow 3d$ transition is an extremely sensitive probe of 4*p* mixing, which results from non-centrosymmetric distortions of the metal complex.

References

1. D. S. McClure, in *Electronic States of Inorganic Compounds: New Experimental Techniques*, edited by P. Day (D. Reidel, Boston, 1974).
2. (a) S. P. Cramer and K. O. Hodgson, *Prog. Inorg. Chem.* **25**, 1 (1979).
(b) P. A. Lee, P. H. Citrin, P. Eisenberger, and B. M. Kincaid, *Rev. Mod. Phys.* **53**, 769-806 (1981).
3. F. C. Brown, in *Synchrotron Radiation Research*, edited by H. Winick and S. Doniach (Plenum Press, New York, 1980), Chapter 4.
4. C. R. Natoli, EXAFS and Near Edge Structure, *Chemical Physics*, edited by A. Bianconi, L. Incoccia, and S. Stipcich, (Springer-Verlag, New York, 1983), Vol. 27, pp. 13-56.
5. H. Winick, in *Synchrotron Radiation Research*, edited by H. Winick and S. Doniach (Plenum Press, New York, 1980), Chapter 2 and Chapter 3.
6. (a) C. D. LuBien, M. E. Winkler, T. J. Thamann, R. A. Scott, M. S. Co, K. O. Hodgson, and E. I. Solomon, *J. Am. Chem. Soc.* **103**, 7014-7016 (1981).

- (b) J. E. Hahn, M. S. Co, D. J. Spira, K. O. Hodgson, and E. I. Solomon, *Biochem. Biophys. Res. Comm.* **112**, 737-745 (1983).
- (c) V. W. Hu, S. I. Chan, G. S. Brown, *Proc. Nat. Acad. Sci. USA* **74**, 3821-3825 (1977).
- (d) J. M. Brown, L. Powers, B. Kincaid, J. A. Larrabee, and T. B. Spiro, *J. Am. Chem. Soc.* **102**, 4210-4216 (1980).
7. J. E. Hahn, R. A. Scott, K. O. Hodgson, S. Doniach, S. R. Desjardins and E. I. Solomon, *Chem. Phys. Lett.*, **88**, 595-598 (1982).
8. (a) C. A. Bates, W. S. Moore, K. J. Standley, and K. W. H. Stevens, *Proc. Phys. Soc.* **79**, 73 (1962).
- (b) M. Sharnoff, *J. Chem. Phys.* **42**, 3383 (1965).
9. J. E. Penner-Hahn, K. O. Hodgson, and E. I. Solomon, manuscript in preparation.
10. R. A. Bair and W. A. Goddard, *Phys. Rev.* **B22**, 2767 (1980).
11. T. A. Smith, M. Berding, J. E. Penner-Hahn, S. Doniach, and K. O. Hodgson, manuscript in preparation.

VI. PHOTOELECTRON SPECTROSCOPY

A. Basic Principles

Photoelectron spectroscopy (PES) provides a powerful probe of the energy level diagram of a metal complex, down to binding energies on the order of 1000 eV (Figure VI-1).¹ This method complements the methods discussed in preceding sections in that rather than measuring the energy and number of photons absorbed due to excitation of electrons into unoccupied bound states or the continuum, PES measures the kinetic energy (E_k) and number of electrons ejected upon photoexcitation into the continuum (referred to as photoemission). For a photon of fixed energy $h\nu$, the kinetic energy of the ejected electron is given by the Einstein relation,

$$E_k = h\nu - E_B. \quad (\text{VI-1})$$

Most research in PES is directed toward determining the binding energies (E_B) of electrons in the energy levels of a metal complex. Usually, the photon sources available for PES have fixed values of $h\nu$ and thus photoelectron spectroscopy is subdivided into two fields, XPS (x-ray photoelectron spectroscopy) and UPS (ultraviolet photoelectron spectroscopy), based on the type and thus energy regime of the source used. (With the availability of continuously tunable synchrotron radiation, this distinction is becoming less clear.)